EPJ Web of Conferences **149**, 05003 (2017) DOI: 10.1051/epjconf/201714905003
10th International Workshop 2017 "Strong Microwaves and Terahertz Waves: Sources and Applications"

Terahertz Bessel beams with orbital angular momentum: diffraction and interference

Yu.Yu. Choporova[1,2], B.A. Knyazev[1,2], N.D. Osintseva[1,3], V.S. Pavelyev[4], B.O. Volodkin[4]

[1]Budker Institute of Nuclear Physics, Novosibirsk, Russia, author@instphys.zz
[2]Novosibirsk State University, Novosibirsk, Russia
[3]Novosibirsk State Technical University, Novosibirsk, Russia
[4]Samara National Research University, Samara, Russia

The fact that light beams are able to carry a mechanical angular momentum is well-known. In paraxial beams, angular momentum can be represented as a sum of the spin (SAM) and orbital (OAM) angular momentum. After paper Allen et al. [1], a lot of articles devoted to the generation, study and the use of beams with orbital angular momentum, or "vortex beams", have been published. To date, vortex beams were obtained in the range from radio frequencies [2] to the soft X-ray radiation [3]. Nevertheless, there are only five studies [4–8], in which vortex beams in the terahertz range have been generated.

Recently, using radiation of the Novosibirsk free electron laser [9] and silicon binary spiral phase axicons, terahertz Bessel beams with OAM with topological charges $l = \pm 1$ and $l = \pm 2$ have been generated for the first time [7]. The intensity distributions of the beams formed by the axicons are in good agreement with the distributions calculated for Bessel beams, but they are identical for both left-handed and right-handed helicities. To determine the characteristics of the beams associated with their rotation, we applied classical experiments on diffraction and interference, adapting them to the terahertz range.

A direct method of detecting the rotation of a beam was its diffraction on a half-plane (Fig. 1, a). Similar experiments with Laguerre-Gaussian and Bessel vortex beams were performed in the visible region in [11], where for the Bessel beams only qualitative results were obtained because of the short laser wavelength and the tiny interference pattern.

In Fig. 1, b the diffraction patterns calculated numerically at several distances are shown. In the experiments, a 16.32×12.24 mm^2 microbolometer array (MBA) with pixel size of 0.051 mm was used as a detector for imaging of diffraction pattern. Because of geometrical restrictions, only planes located at a distance z of more than 35 mm could be recorded. The recorded patterns were identical with the calculated ones.

The diffraction patterns shown in Fig. 1 clearly demonstrate the rotation of the beam. According to the theory [12], the rate of change of azimuthal angle of the trajectory of the Poynting vector with z is given by

$$\frac{d\alpha}{dz} = \frac{1}{\rho}\frac{S_\varphi}{S_z} = \frac{l}{k\rho^2}, \tag{1}$$

where $\rho = (x^2 + y^2)^{1/2}$ and S_φ, S_z are the components of the Poynting vector that is normal to the helical wavefront. Since the speed of the azimuthal rotation is inversely proportional to the square of the radius, the inner ring rotates most rapidly after the obstacle. The Poynting vector makes a complete revolution along the helix at the distance

$$\Delta z_{pitch} = \frac{2\pi k \rho^2}{l}. \tag{2}$$

From experiments and calculations it follows that one turn of the Poynting vector is 240 mm for the first ring and 340 mm for the second one. The direction of rotation corresponds to the sign of the topological charge.

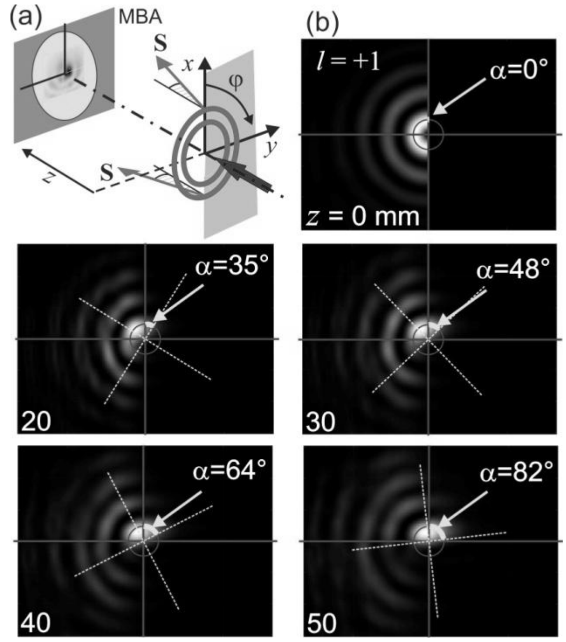

Fig. 1. Diffraction of vortex beams ($\lambda = 141$ μm) on a half-plane: (a) experimental schematic; (b) diffraction patterns for beam with the topological charge $l = +1$ vs. distance D. Radii of first and second beam rings were 0.9 mm and 1.9 mm, respectively

A simpler method for determining the twist parameters of a beam is the double slit Young experiment (Fig. 2, a). To determine all the beam parameters, it requires recording only one diffraction pattern at some distance z from the slits. Because in any plane $z = const$ the beam phase grows up with the azimuthal angle as $\Phi = l\varphi$, interference fringes become distorted. Simple calculations show that the maxima of the intensity of the fringes are described by an equation, the notation in which is clear from Fig. 2

$$x(y) = -a \tan\left[\frac{2\pi a y}{l z \lambda} + \frac{m\pi}{l} + \frac{\pi}{2}\right], \quad m = 0 \ldots l-1. \tag{3}$$

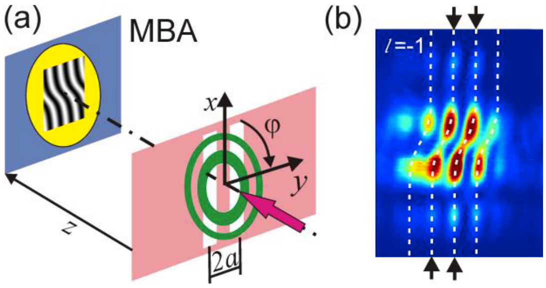

Fig. 2. (a) Schematic of double-slit experiment. (b) Diffraction pattern recorded for vortex beam with topological charge $l=-1$ at $\lambda=141$ µm

The Bessel beam of a free-electron laser with topological charge -1, expanded five times by a telescopic system, illuminated two slits located at a distance of 4 mm. The dotted curves calculated using Eq. (3) are superimposed on the diffraction pattern (Fig. 2, b), recorded by the microbolometer matrix at a distance of 60 mm. For the beam with a charge equal to -2, the bending of the curves increased, and the shift of the bands from the upper edge to the lower edge of the frame increased by a factor of two. When the direction of rotation of the beam changed, the slope of the bands changed to the opposite.

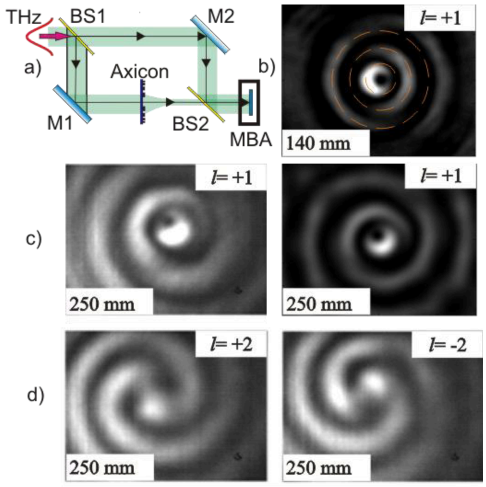

Fig. 3. Interference of vortex and Gaussian beams. (*a*) Mach–Zehnder interferometer; (*b*) interference of Bessel and Gauss beams at different distances from axicon. The dashed rings indicate the maxima of the intensity of the Bessel beam. Left column – experimental data; right column – similations

Bessel beams bounded in the aperture, formally speaking, are not diffractive at a certain distance. Investigation of the interference of the beams obtained with Gaussian wave in the Mach-Zehnder interferometer (Fig. 3, a) made it possible to reveal the details of the decay of the Bessel beam, which begins already in the process of its propagation.

This fact becomes obvious if we observe a change in the interference pattern with the distance (Fig. 3, b–d). The phase of adjacent rings of Bessel beams differs by a value of π, and the phase increases along the rings from 0 to $2\pi l$. The wave front of the Gaussian beam was practically flat. At a distance z = 140 mm, the interference along the rings varies in azimuth l times from constructive to destructive, which indicates that the wave front in this Bessel beam is practically flat. At a distance of 250 mm, the interference pattern changes, forming spirally divergent bands. Since the wavefront of a Gaussian laser beam at such a small distance remains practically unchanged, this indicates the beginning of the transformation of the helicoidal wave front into conically divergent plane waves. The number of spirals and their direction also make it possible to determine the magnitude and sign of the topological charge of the beam.

Acknowledgments

Experiments were supported by RFBR grant 15-02-06444. The axicons were fabricated under supported by the Ministry of Education and Science of the Russian Federation (project 16.7894.2017/6.7). The terahertz beamline was designed under support of RSF grant 14-50-00080. The experiments engaged equipment belonging to the Siberian Synchrotron and Terahertz Radiation Center.

References

1. *Allen, L., Beijersbergen, M.W., Spreeuw, R.J.C., Woerdman, J.P.* Orbital angular momentum of light and the transformation of Laguerre–Gaussian laser modes. Phys. Rev. 1992. V. A 45. P. 8185–8189.
2. *Thide, B., Then, H., Sjoholm, J., Palmer, K., Bergman, J., Carozzi, T.D., Istomin, Y.N., Ibragimov, N.H., Khamitova, R.* Utilization of Photon Orbital Angular Momentum in the Low-Frequency Radio Domain // Phys. Rev. Lett. 2007. V. 99. 087701.
3. *Bahrdt, J., Holldack, K., Kuske, P., Mueller, R., Scheer, M., Schmid, P.* First Observation of Photons Carrying Orbital Angular Momentum in Undulator Radiation // Phys. Rev. Lett. 2013. V. 111. 034801.
4. *He, J., Wang, X., Hu, D., Ye, J., Feng, S., Kan, Q., Zhang, Y.* Opt. Express, 2013. V. 21. P. 20230-20239.
5. *Miyamoto, K., Suizu, K., Akiba, T., Omatsu, T.* Direct observation of the topological charge of a terahertz vortex beam generated by a Tsurupica spiral phase plate // Appl. Phys. Lett. 2014. 104. 261104.
6. *Imai, R., Kanda, N., Higuchi, T., Konishi, K., Kuwata-Gonokami, M.* Generation of broadband terahertz vortex beams // Opt. Lett. 2014. V. 39. P. 3714-3417.
7. *Knyazev, B.A., Choporova, Yu.Yu., Mitkov, M.S., Pavelyev, V.S., Volodkin, B.O.* Generation of Terahertz surface plasmon polaritons using nondiffractive Bessel beams with orbital angular momentum // Phys. Rev. Lett. 2015. V. 115. 163901.
8. *Wei, X., Liu, C., Niu, L., Zhang, Z., Wang, K., Yang, Z., Liu, J.* Generation of arbitrary order Bessel beams via 3D printed axicons at the terahertz frequency range // Appl. Opt. 2015. V. 54. P. 10641-10649.
9. *Kulipanov, G.N., et al*. Novosibirsk Free Electron Laser—Facility Description and Recent Experiments // IEEE Trans. Terahertz Sci. Technol. 2015. V. 5. P. 798-809.
10. *Arlt, J.* Handedness and azimuthal energy flow of optical vortex beams // J. Modern Opt. 2003.V. 50, P. 1573-1580.
11. *Allen, L., Padgett, M.J.* The Poynting vector in Laguerre±Gaussian beams and the interpretation of their angular momentum density // Optics Communs. 2000. V. 184. P. 67-71.
12. *Emile, O., Emile, J.* Young's double-slit interference pattern from a twisted beam. // Appl. Physics B - Laser and Optics, Springer Verlag. 2014. V. 117. P. 487-491.